

## Adducts of Titanium Tetrahalides with Neutral Lewis Bases. Part I. Structure and Stability: a Vibrational and Multinuclear NMR Study

ERIC TURIN\*, ROGER M. NIELSON and ANDRÉ E. MERBACH\*\*

Institut de Chimie Minérale et Analytique, Université de Lausanne, 3, Place du Château, CH-1005 Lausanne, Switzerland

(Received February 20, 1987)

### Abstract

Raman, infra-red and multinuclear NMR spectroscopy were used to establish the structure of several  $\text{TiX}_4 \cdot 2\text{L}$  adducts ( $\text{X} = \text{F}, \text{Cl}, \text{Br}$ ;  $\text{L} = \text{Lewis base}$ ) in inert solvents. In contrast to the analogous  $\text{SnX}_4 \cdot 2\text{L}$  adducts where a *cis*–*trans* equilibrium prevails, most of the  $\text{TiX}_4 \cdot 2\text{L}$  adducts studied were found to have only the *cis* configuration. *Trans* isomers were observed but their formation was dependent on the donor ability of the ligand. In dichloromethane solution, the adducts with  $\text{L} = \text{Me}_2\text{O}, \text{Me}_2\text{S}, (\text{MeOCH}_2)_2, \text{Et}_2\text{S}, \text{THT}, \text{Me}_2\text{Se}, \text{MeCN}, \text{Me}_2\text{CO}, \text{Cl}(\text{MeO})_2\text{PO}, \text{Cl}_2(\text{MeO})\text{PO}, \text{Cl}_3\text{PO}$  and  $\text{Cl}_2(\text{Me}_2\text{N})\text{PO}$  were found to have the *cis* configuration only. For the adducts with  $\text{L} = \text{THF}, \text{Cl}(\text{Me}_2\text{N})_2\text{PO}$  and  $\text{TMPA}$ , a *cis*–*trans* equilibrium was observed. The thermodynamic parameters were measured for *cis*–*trans* isomerization for  $\text{TiCl}_4 \cdot 2\text{TMPA}$  in  $\text{CHCl}_3$ ; these parameters are:  $K_{\text{iso}}^{277} = [\textit{trans}]/[\textit{cis}] = 0.36$ ,  $\Delta H_{\text{iso}}^\circ = -1.3 \pm 1.3$  kJ/mol,  $\Delta S_{\text{iso}}^\circ = -13.1 \pm 7.5$  J/mol K, and  $\Delta V_{\text{iso}}^\circ = -1.3 \pm 0.8$  cm<sup>3</sup>/mol. A complex equilibrium involving *cis* and *trans* isomers and the ionic complex  $[\text{TiCl}_3 \cdot 3\text{HMPA}]\text{Cl}$  was found to occur for the  $\text{TiCl}_4$  adduct with  $\text{L} = \text{HMPA}$ . <sup>1</sup>H NMR was used to establish the relative stabilities of the *cis* adducts and the following sequence was obtained:  $\text{Me}_2\text{O} \sim \text{MeCN} < \text{Me}_2\text{CO} < \text{Me}_2\text{S} < \text{Me}_2\text{Se} \ll \text{Cl}(\text{MeO})_2\text{PO} \ll \text{TMPA} < \text{Cl}(\text{Me}_2\text{N})_2\text{PO}$ .

### Introduction

We have, for a number of years now, been interested in the ligand exchange kinetics of octahedral metal complexes in which the metal is in a high oxidation state. Of particular interest to us is the exchange of Lewis base ligands between free and coordinated sites on group IV and V metal halide systems [1]. In this area we have completed studies

on  $\text{MX}_5\text{L}$  ( $\text{M} = \text{Nb}, \text{Ta}$  [2],  $\text{Sb}$  [3];  $\text{X} = \text{F}, \text{Cl}, \text{Br}$ ;  $\text{L} = \text{Lewis base}$ ) and  $\text{SnX}_4 \cdot 2\text{L}$  [4] adducts. These systems are particularly attractive since the ligand exchange process occurs in a single step, making mechanistic assignments much easier. We are now extending the available kinetic data to include the group IVB metal tetrahalide Lewis base adducts: specifically,  $\text{TiX}_4 \cdot 2\text{L}$ .

The  $\text{TiX}_4 \cdot 2\text{L}$  adducts can exist in both *cis* and *trans* configurations. Numerous structural studies have been undertaken during the last 20 years in order to determine which isomer, if any, predominates. The technique used most often in these endeavours is vibrational spectroscopy. A powerful structure determination method, vibrational spectroscopy permits the unambiguous identification of *cis* and *trans* isomers. However, the concentration of the isomers needs to be great enough to produce observable bands in the spectrum; this is especially important because the bands often overlap, obscuring the presence of weak bands. NMR spectroscopy complements the information obtained from vibrational spectroscopy in that the presence of a small quantity of an isomer can be established and the relative concentrations of the isomers can be measured. NMR has been utilized to a small degree in the characterization of  $\text{TiX}_4 \cdot 2\text{L}$  adducts (especially <sup>19</sup>F NMR), but it has not been used to the extent necessary to gain a firm understanding of  $\text{TiX}_4 \cdot 2\text{L}$  coordination chemistry.

From the vibrational, crystal structure and NMR data that exist for  $\text{TiX}_4 \cdot 2\text{L}$  adducts it is becoming increasingly clear that the structures of the adducts do not parallel those of the analogous  $\text{SnX}_4 \cdot 2\text{L}$  adducts. Most studies have shown that only the *cis*- $\text{TiX}_4 \cdot 2\text{L}$  isomer [5] exists for many Lewis base ligands although the  $\text{SnX}_4 \cdot 2\text{L}$  adducts [6] containing the same ligands exist in both *cis* and *trans* configurations. In this paper we combine the use of vibrational spectroscopy (both Raman and IR) with multinuclear NMR spectroscopy (<sup>1</sup>H, <sup>13</sup>C, <sup>19</sup>F, <sup>31</sup>P) to determine the structures of a series of  $\text{TiX}_4 \cdot 2\text{L}$  adducts containing a number of Lewis base ligands. This provides the necessary structural framework for the kinetic study reported in the following paper.

\*Taken, in part, from the Ph.D. Thesis of E.T.

\*\*Author to whom correspondence should be addressed.

## Experimental

### Sample Preparation

To prevent hydrolysis of  $\text{TiX}_4$  and the  $\text{TiX}_4 \cdot 2\text{L}$  adducts with atmospheric water, all manipulations were performed in a glove box containing less than 6 ppm water. The various Lewis base ligands and the solvents were dried and distilled under argon using standard methods and were stored over molecular sieves. Chloroform was purified by passing it over a 60 cm column containing basic  $\text{Al}_2\text{O}_3$ .  $\text{TiCl}_4$  (Fluka > 99%),  $\text{TiF}_4$  (ROC/RIC 99%) and dimethylselenium (Strem Chemical) were used without further purification.  $\text{TiBr}_4$  (Merck) was sublimed at room temperature at  $10^{-3}$  torr.

The solid adducts used in the vibrational studies were prepared by mixing dichloromethane solutions of  $\text{TiX}_4$  with a solution of the Lewis base in 1:4 molar ratio and then either evaporating the mixture to a solid or crystallizing the product in the presence of *n*-pentane at low temperature. The products were kept at  $5 \times 10^{-2}$  torr for 15 min and sealed in Pyrex tubes under vacuum. Microanalyses were performed by A. Bernhardt, 5251 Elbach-über-Engelskirchen, F.R.G. and the results were in excellent agreement with the calculated values.

Solutions of the samples were prepared by mixing the necessary quantities of 10%  $\text{TiX}_4$  and 10% Lewis base solutions and by diluting with the necessary solvent. For vibrational work the solvent was  $\text{CH}_2\text{Cl}_2$ ,  $\text{CH}_2\text{Br}_2$ ,  $\text{CHBr}_3$  or  $\text{CH}_3\text{NO}_2$  and for NMR work the solvent was mixtures of deuterated and normal  $\text{CH}_2\text{Cl}_2$ ,  $\text{CHCl}_3$  or  $\text{CH}_3\text{NO}_2$ . The solutions were prepared to have a  $\text{TiX}_4 \cdot 2\text{L}$  concentration of 0.025 to 0.20 mol  $\text{kg}^{-1}$  and a  $[\text{TiX}_4 \cdot 2\text{L}]:[\text{free ligand}]$  ratio of 1:2.

### Vibrational Measurements

Raman spectra were recorded between 600 and 50  $\text{cm}^{-1}$  on a 1403 SPEX spectrometer using the 647 nm line of a krypton laser. The solution adducts were contained in capillary tubes or, in the case of  $\text{TiCl}_4 \cdot 2\text{Me}_2\text{Se}$ , a rotating cell. The 218  $\text{cm}^{-1}$  band of  $\text{CCl}_4$  was used for instrument calibration. Infrared spectra were recorded between 600 and 200  $\text{cm}^{-1}$  using a Perkin-Elmer 577 instrument purged with  $\text{N}_2$ . The samples were prepared in Nujol and the spectra were collected on CsBr plates. The  $\text{TiBr}_4 \cdot 2\text{L}$  adducts are highly colored and, consequently, the Raman spectra could not be obtained due to the absorption of the light source and subsequent decomposition of the adducts.

### NMR Spectroscopy

Ambient pressure proton and  $^{13}\text{C}\{^1\text{H}\}$  NMR spectra were obtained using a Bruker WP-60 spectrometer operating at 60.00 and 15.09 MHz, respectively.  $^{31}\text{P}\{^1\text{H}\}$  and  $^{19}\text{F}$  NMR spectra were collected

with a Bruker HX-90 instrument operating at 36.43 and 84.67 MHz, respectively. The field was locked using the deuterium signal of the solvent and the temperature was measured with a substitution technique using a platinum resistor [7]. Variable pressure proton NMR experiments were performed at 200.0 MHz on a Bruker CXP-200 instrument without a field lock as described previously [8]. The field inhomogeneity for the pressure measurements was in the order of 1–4 Hz. The chemical shift values are reported using the high frequency positive convention and are referenced to TMS for  $^1\text{H}$  and  $^{13}\text{C}$ ,  $\text{CFCl}_3$  for  $^{19}\text{F}$ , and 62.5%  $\text{H}_3\text{PO}_4$  for  $^{31}\text{P}$ .

## Results

### Vibrational Study

In principle,  $\text{TiX}_4 \cdot 2\text{L}$  Lewis base adducts can exist in two isomeric forms: one with the Lewis base ligands located in *cis* position and the other with the ligands in *trans* position. If the symmetry of the ligand is ignored and is considered as a point mass, the *cis* and *trans* isomers belong to the  $C_{2v}$  and  $D_{4h}$  point group, respectively. The vibrational representation for  $C_{2v}$  symmetry is:

$$\Gamma_{C_{2v}} = 6A_1 + 2A_2 + 3B_1 + 4B_2$$

of which  $2A_1 + B_1 + B_2$  represent Ti–X bond stretches and  $A_1 + B_2$  represent stretches of the Ti–L bonds. The  $A_1$ ,  $B_1$  and  $B_2$  vibrational modes are both Raman and IR active.

For  $D_{4h}$  symmetry the vibrational representation is:

$$\Gamma_{D_{4h}} = 2A_{1g} + B_{1g} + B_{2g} + E_g + 2A_{2u} + B_{2u} + 3E_u$$

of which  $A_{1g} + B_{1g} + E_u$  represent Ti–X bond stretches and  $A_{1g} + A_{2u}$  represent Ti–L stretching vibrations. Of the stretching modes,  $A_{1g}$  and  $B_{1g}$  are Raman active and  $A_{2u}$  and  $E_u$  are IR active. Since the  $D_{4h}$  point group is centrosymmetric, the mutual exclusion rule applies.

The results of the Raman experiments on solutions of the  $\text{TiCl}_4 \cdot 2\text{L}$  adducts showed that the number of polarized bands corresponding to Ti–Cl stretchings in each spectrum varied from one to three depending on the adduct. One polarized band was observed for  $\text{L} = \text{HMPA}$ , two were observed for  $\text{L} = \text{Me}_2\text{O}$ ,  $\text{Me}_2\text{S}$ ,  $(\text{MeOCH}_2-)_2$ ,  $\text{Et}_2\text{S}$ ,  $\text{THT}$ ,  $\text{Me}_2\text{Se}$ ,  $\text{Me}_2\text{CO}$ ,  $\text{Cl}(\text{MeO})_2\text{-PO}$ ,  $\text{Cl}_2(\text{MeO})\text{PO}$ ,  $\text{Cl}_3\text{PO}$  and  $\text{Cl}_2(\text{Me}_2\text{N})\text{PO}$  and three polarized bands were observed for  $\text{L} = \text{THF}$  and  $\text{TMPA}$ . Beattie *et al.* [9] have made a normal coordinate analysis for *cis* and *trans* species of the type  $\text{MX}_4 \cdot 2\text{L}$ . Using the results from their calculations, the mutual exclusion rule for the *trans* isomer, and the fact that the symmetric vibrations will be polarized in solution, allow us to assign the frequencies of the stretching vibrations. The adducts having

TABLE I. Ti-Cl Raman Vibrational Frequencies ( $cm^{-1}$ ) for Several  $TiCl_4 \cdot 2L$  and  $TiCl_4 \cdot L-L$  Adducts in Solution<sup>a</sup>

Ligand <sup>b</sup>	<i>cis</i> <sup>c</sup>		<i>trans</i> <sup>c</sup> $\nu_1(A_{1g})$	Reference <sup>d</sup>
	$\nu_1(A_1)$	$\nu_2(A_1)$		
Me <sub>2</sub> O	393(100)	313(95)		
THF <sup>e</sup>	384(100)	306(80)	322(75)	27
(MeOCH <sub>2</sub> -) <sub>2</sub>	394(100)	306(38)		
Me <sub>2</sub> S	388(45)	318(100)		28
Et <sub>2</sub> S	378(55)	310(100)		
THT <sup>f</sup>	386(46)	316(100)		31
Me <sub>2</sub> Se	388(38)	311(100)		
Me <sub>2</sub> CO	391(100)	312(74)		27
TMPA <sup>g</sup>	364(100)	299(44)	305(41)	
Cl(MeO) <sub>2</sub> PO	378(100)	292(38)		
Cl <sub>2</sub> (MeO)PO	396(100)	303(21)		
Cl <sub>3</sub> PO	396(100)	314(79)		29
Cl <sub>2</sub> (Me <sub>2</sub> N)PO	389(100)	305(53)		
HMPA <sup>h</sup>			300(100)	30

<sup>a</sup> All the spectra were recorded in CH<sub>2</sub>Br<sub>2</sub> except for L = Me<sub>2</sub>O, which was recorded in CH<sub>2</sub>Cl<sub>2</sub>, and L = HMPA in CHBr<sub>3</sub>. <sup>b</sup> All ligands listed are monodentate except for (MeOCH<sub>2</sub>-)<sub>2</sub>, which is bidentate. <sup>c</sup> The values in parentheses are the relative intensities of the polarized Raman bands. <sup>d</sup> The references listed are representative samples of vibrational studies reported in the literature. <sup>e</sup> THF = tetrahydrofuran. <sup>f</sup> THT = tetrahydrothiophen. <sup>g</sup> TMPA = (MeO)<sub>3</sub>PO. <sup>h</sup> HMPA = (Me<sub>2</sub>N)<sub>3</sub>PO.

two polarized Raman bands can be immediately assigned as having the *cis* configuration since the Raman active *cis* modes  $\nu_1(A_1)$  and  $\nu_2(A_1)$  are expected to be polarized and to have corresponding absorbances in the IR, as observed. The assignment of the Raman active bands for the adducts having *cis* geometry is given in Table I. In the presence of a small excess of free ligand, the adduct  $TiCl_4 \cdot 2HMPA$  had only one polarized Raman band at 300  $cm^{-1}$ . The configuration of this adduct was therefore assigned as being *trans* and the 300  $cm^{-1}$  band was assigned as being the  $A_{1g}$  mode. The presence of three polarized bands for the adducts with L = THF and TMPA indicates that both *cis* and *trans* isomers exist in solutions of these adducts. To make the necessary band assignments, the following procedure was used. Since the *cis* isomer is unsymmetrical it should possess a dipole moment and its formation should be facilitated in solvents with increasing polarity. We recorded the Raman spectrum of  $TiCl_4 \cdot 2L$ , L = THF and TMPA in three solvents of varying dielectric constant: CHBr<sub>3</sub> ( $\epsilon = 4.4$ ), CH<sub>2</sub>Br<sub>2</sub> ( $\epsilon = 7.4$ ) and CH<sub>3</sub>NO<sub>2</sub> ( $\epsilon = 35.9$ ). For L = THF the relative intensity of the 306  $cm^{-1}$  band to the one at 322  $cm^{-1}$  increased from a value of 0.92 in CHBr<sub>3</sub>, to 1.07 in CH<sub>2</sub>Br<sub>2</sub> and to 4.30 in CH<sub>3</sub>NO<sub>2</sub>. However, the relative intensities of the 384 and 306  $cm^{-1}$  bands remained constant, showing that the 322  $cm^{-1}$  band is due to the *trans* isomer since its intensity decreases as the solvent polarity increases. The frequencies of the polarized bands for L = TMPA were assigned in a similar manner and are summarized in Table I. Figure 1 shows the Raman spectra of  $TiCl_4 \cdot 2TMPA$  in

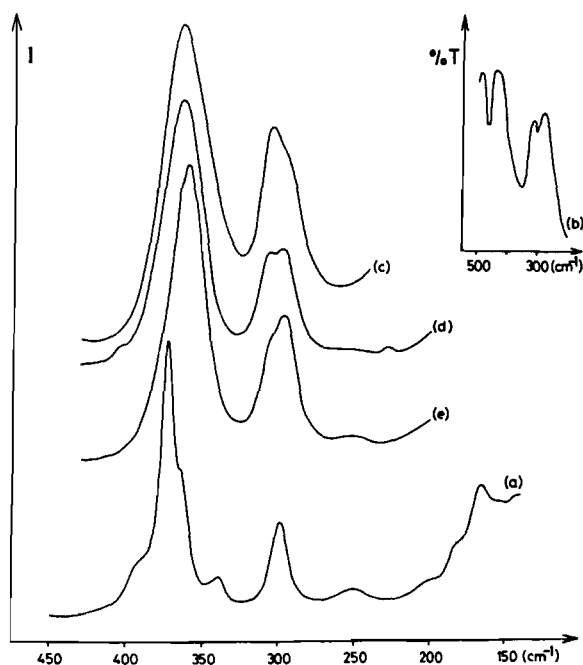


Fig. 1. Raman (a) and infra-red (b) spectra of solid  $TiCl_4 \cdot 2TMPA$  and Raman spectra of  $TiCl_4 \cdot 2TMPA$  in CHBr<sub>3</sub> (c), CH<sub>2</sub>Br<sub>2</sub> (d) and CH<sub>3</sub>NO<sub>2</sub> (e).

several solvents showing the decrease in intensity of the 305  $cm^{-1}$  band with respect to those at 364 and 299  $cm^{-1}$  as the solvent polarity increases.

To summarize the results of the vibrational study of  $TiCl_4 \cdot 2L$  adducts in solution, only the *trans* isomer was found for L = HMPA, only the *cis* isomer exists for

TABLE II.  $^1\text{H}$  NMR Chemical Shifts  $\delta^a$ , Chemical Shift Differences  $\Delta\delta^b$  and Stoichiometries for *cis*- $\text{TiX}_4 \cdot 2\text{L}$  and *cis*- $\text{TiCl}_4 \cdot \text{L} - \text{L}$  in  $\text{CH}_2\text{Cl}_2$ 

Adduct	$\delta$ $\pm 0.01$ (ppm)	$\Delta\delta$ $\pm 0.01$ (ppm)	Stoichiometry Ti:L	$[\text{Ti}]_{\text{T}}$ (mol kg $^{-1}$ )	$[\text{L}]_{\text{T}}$ (mol kg $^{-1}$ )	$T$ (K)
<i>cis</i> - $\text{TiCl}_4 \cdot 2\text{L}$						
$\text{Me}_2\text{O}$	4.06	0.74	1:1.97	0.10	0.49	175
$\text{Me}_2\text{S}$	2.62	0.49	1:1.96	0.05	0.20	173
$(\text{CH}_3\text{CH}_2)_2\text{S}^c$	1.40	0.15	1:1.96	0.10	0.43	173
$(\text{CH}_3\text{CH}_2)_2\text{S}^c$	3.14	0.54	1:1.96	0.10	0.43	173
$\text{Me}_2\text{Se}^d$	2.55	0.54	1:1.97	0.10	0.40	186
$\text{MeCN}$	2.56	0.46	1:1.96	0.025	0.10	176
$\text{Me}_2\text{CO}$	2.75	0.50	1:2.04	0.05	0.20	176
<i>cis</i> - $\text{TiCl}_4 \cdot \text{L} - \text{L}$						
$(\text{MeOCH}_2-)_2$	4.10	0.76	1:1.08	0.07	0.21	243
$(\text{MeOCH}_2-)_2$	4.32	0.83	1:1.08	0.07	0.21	243
<i>cis</i> - $\text{TiBr}_4 \cdot 2\text{L}$						
$\text{Me}_2\text{S}$	2.68	0.55	1:1.94	0.05	0.20	173
$\text{Me}_2\text{Se}$	2.62	0.60	1:1.98	0.05	0.20	173

<sup>a</sup>Internal reference was TMS. <sup>b</sup> $\Delta\delta = \delta(\text{TiCl}_4 \cdot 2\text{L}) - \delta(\text{L})$ . <sup>c</sup> $^3J(^1\text{H}-^1\text{H}) = 7.0$  Hz for the coordinated ligand and 7.2 Hz for the free ligand. <sup>d</sup> $^2J(^1\text{H}-^{77}\text{Se}) = 7.2$  Hz for the coordinated ligand and 9.9 Hz for the free ligand.

L =  $\text{Me}_2\text{O}$ ,  $(\text{MeOCH}_2-)_2$ ,  $\text{Me}_2\text{S}$ ,  $\text{Et}_2\text{S}$ , THT,  $\text{Me}_2\text{Se}$ ,  $\text{Me}_2\text{CO}$ ,  $\text{Cl}(\text{MeO})_2\text{PO}$ ,  $\text{Cl}_2(\text{MeO})\text{PO}$ ,  $\text{Cl}_3\text{PO}$  and  $\text{Cl}_2-(\text{Me}_2\text{N})\text{PO}$  and finally, both *cis* and *trans* isomers were observed for L = THF and TMPA.

### NMR Spectroscopy

All the solutions of  $\text{TiX}_4 \cdot 2\text{L}$  used in the NMR study contained an equimolar excess of free ligand with respect to coordinated ligand. At room temperature, chemical exchange between free and coordinated ligands is generally too rapid to allow observation of both peaks in the NMR spectrum; therefore, it was necessary to perform the NMR experiments at a temperature low enough to block the exchange process.

The  $^1\text{H}$  NMR spectra of  $\text{TiCl}_4 \cdot 2\text{L}$ , L =  $\text{Me}_2\text{O}$ ,  $\text{Me}_2\text{S}$ ,  $\text{Et}_2\text{S}$ ,  $\text{Me}_2\text{Se}$ ,  $\text{CH}_3\text{CN}$ ,  $\text{Me}_2\text{CO}$  and  $(\text{MeOCH}_2-)_2$  and  $\text{TiBr}_4 \cdot 2\text{L}$ , L =  $\text{Me}_2\text{S}$  and  $\text{Me}_2\text{Se}$  were recorded in  $\text{CH}_2\text{Cl}_2/\text{CD}_2\text{Cl}_2$  and are reported in Table II. All the spectra had two peaks or, in the situations where spin-spin coupling with  $^1\text{H}$  occurs, two groups of peaks corresponding to the coordinated and free forms of the ligand. The signal due to the coordinated ligands was always shifted downfield from the free ligand peak position, this being indicative of the electron donating nature of the Lewis base ligand when it is coordinated to the titanium. Integration of the NMR signals permits the stoichiometry (Ti:L) of the  $\text{TiX}_4 \cdot 2\text{L}$  adduct to be calculated. These results are given in Table II and they show that the stoichiometry is two for the adducts with monodentate ligands and one for the bidentate ligand  $(\text{MeOCH}_2-)_2$ .

Based on the fact that: (i) only two types of ligands were observed in the NMR spectra, (ii) the observed stoichiometry agrees with the expected value for the presence of only one isomer, and (iii) the vibrational data show only the presence of the *cis* isomer, we conclude that in  $\text{CH}_2\text{Cl}_2/\text{CD}_2\text{Cl}_2$  solutions of  $\text{TiCl}_4 \cdot 2\text{L}$  adducts with an excess of free ligand only the *cis* isomer is present for L =  $\text{Me}_2\text{O}$ ,  $\text{Me}_2\text{S}$ ,  $\text{Et}_2\text{S}$ ,  $\text{Me}_2\text{Se}$ ,  $\text{MeCN}$ ,  $\text{Me}_2\text{CO}$  and  $(\text{MeOCH}_2-)_2$ . Although no vibrational data are available for the  $\text{TiBr}_4 \cdot 2\text{L}$  adducts, the chemical shift values [16] lead us to conclude that only the *cis* isomer is present for L =  $\text{Me}_2\text{S}$  and  $\text{Me}_2\text{Se}$ .

As mentioned above, ligand exchange between free and coordinated sites was observed at different temperatures depending on the lability of the ligand. For the labile  $\text{Me}_2\text{O}$  ligand, exchange is observed at 170 K, but for the bidentate ligand  $(\text{MeOCH}_2-)_2$ , exchange is not observed until 263 K. The decreased lability of the  $(\text{MeOCH}_2-)_2$  ligand is probably due to the fact that exchange between free and complexed ligands requires the breaking of two Ti-O bonds whereas exchange of the monodentate ligands only requires the breaking of one bond.

A recent study on  $\text{SO}_2$  solutions of  $\text{TiCl}_4$  and  $\text{Me}_2\text{O}$  described the observation of both the *trans* and the *cis* isomers of  $\text{TiCl}_4 \cdot 2\text{Me}_2\text{O}$  [10]. The authors reported that at 189 K and in the presence of excess  $\text{Me}_2\text{O}$ , two NMR peaks were observed in the 100 MHz  $^1\text{H}$  NMR spectrum. One of the two peaks was located at 4.07 ppm and the other peak was

upfield from the first, but its position depended on the concentration of  $Me_2O$  in solution. The 4.07 ppm peak was assigned as being due to coordinated  $Me_2O$  on *trans*- $TiCl_4 \cdot 2Me_2O$  and the other was assigned as being due to a fast exchange average between the free ligand and the coordinated ligands on *cis*- $TiCl_4 \cdot 2Me_2O$ . We did not observe this behavior in the inert solvent  $CH_2Cl_2$ , where only the *cis* isomer is present. In order to shed a little light on this solvent dependence on the structure of the  $TiCl_4 \cdot 2Me_2O$  adducts we performed a limited number of NMR experiments in  $SO_2/CH_2Cl_2$  solvent mixtures. Four samples were prepared with a  $TiCl_4:Me_2O$  ratio of about 1:6 and with the mole percentage of  $SO_2$  being 0, 36, 60 and 100%. From these experiments two observations were noted. First, at 190 K two NMR peaks were observed in the 200 MHz  $^1H$  spectrum for all four samples, one at 4.07 ppm and the other at 3.32 to 3.21 ppm, depending on the solvent composition. Integration of these peaks showed that the calculated stoichiometry, assuming that only one isomer is present, decreases from 2.0 in 0%  $SO_2$  (100%  $CH_2Cl_2$ ), to 1.9 in 36%  $SO_2$ , to 1.7 in 60%  $SO_2$  and to 1.6 in 100%  $SO_2$  (0%  $CH_2Cl_2$ ). Second, the width at half height of the upfield peak increased markedly in the presence of  $SO_2$  ( $W_{1/2} = 0.5$  Hz in  $CH_2Cl_2$  and 8–14 Hz in  $SO_2/CH_2Cl_2$  and  $SO_2$  mixtures) while the 4.07 ppm peak width remained unchanged. Since the calculated stoichiometry decreases from the expected value of 2 when  $CH_2Cl_2$  is replaced with  $SO_2$ , it appears that not all the  $TiCl_4$  in solution forms a single coordinated species. The remaining  $TiCl_4$  could be uncoordinated, but, due to the chemical shift change, it more likely forms another type of  $TiCl_4$  Lewis base adduct. In addition, the broadening of the upfield peak in the presence of  $SO_2$  indicates that some exchange process is occurring between the free ligand molecules and the unknown  $TiCl_4/Me_2O$  adduct, as reported. If the broadening of the upfield peak is due to fast exchange between two ligand sites, then a decrease in temperature should produce a broadening of the NMR signal and, eventually, a separation of the two coalesced signals. The 100%  $SO_2$  sample froze below 189 K but experiments performed at 176 K on the  $CH_2Cl_2/SO_2$  solutions showed that the peak width did increase slightly (up to 4 Hz), indicating that exchange is the source of the broadening. In contrast, the NMR spectrum of the 100%  $CH_2Cl_2$  solution did not change when the temperature was decreased. We conclude that for  $TiCl_4/Me_2O$  mixtures in  $SO_2$  and in  $CH_2Cl_2/SO_2$  mixtures, more than one coordinated form of  $TiCl_4$  exists in solution. One form, with an NMR signal at 4.07 ppm, is probably the *cis* isomer and the other, with an NMR peak upfield from the 4.07 ppm peak, is probably involved in a fast ligand exchange process with the free ligand. The species involved in the exchange process could be the *trans* isomer, the mono coordinate adduct, or a

mixed ligand adduct containing  $Me_2O$  and  $SO_2$ ; its identity has not been established. However, in  $CH_2Cl_2$ , the agreement of the observed stoichiometry with the theoretical value of 2 and the absence of exchange effects on the free ligand signal at very low temperatures, lead us to conclude that only the *cis*- $TiCl_4 \cdot 2Me_2O$  isomer exists in  $CH_2Cl_2$  solution.

For the  $TiBr_4$  adducts with  $Me_2CO$  and MeCN the  $^1H$  NMR spectra at 173 K showed, in addition to the free ligand peak, a signal downfield from the ligand peak as observed for the  $TiCl_4$  adducts. The signals are probably due to the *cis* isomer but integration of them revealed that the coordination number is 1.51 for  $Me_2CO$  and 1.74 for MeCN, indicating that  $TiBr_4$  is not quantitatively forming the 1:2 adduct. A solution of  $TiBr_4$  with  $Me_2O$  produced a red-black precipitate indicative of decomposition of the species.

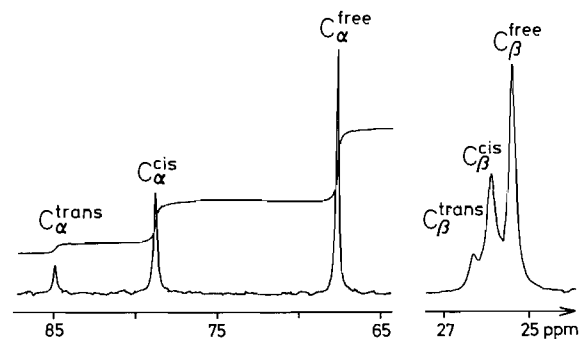


Fig. 2.  $^{13}C\{^1H\}$  NMR spectrum at 200 K of *cis*- and *trans*- $TiCl_4 \cdot 2THF$  in the presence of excess THF and in  $CD_2Cl_2$ .  $[TiCl_4 \cdot 2L] = 0.20$  mol  $kg^{-1}$ ,  $[free\ THF] = 0.70$  mol  $kg^{-1}$ .

Vibrational spectroscopy indicated for the  $TiCl_4 \cdot 2THF$  system that both *cis* and *trans* isomers are in equilibrium in solution. This is confirmed by NMR spectroscopy. Due to the complexity of the  $^1H$  spectrum, we recorded the  $^{13}C\{^1H\}$  NMR spectrum in  $CD_2Cl_2$  at 200 K. The spectrum is shown in Fig. 2 and it confirms the presence of a *cis*-*trans* equilibrium. We have assigned the resonances at 84.9, 78.8 and 67.8 ppm as being due to the  $\alpha$  carbons of the *trans*, *cis* and free ligands, respectively. The three resonances at 26.3, 25.9 and 25.4 ppm are assigned to the  $\beta$  carbons of the *trans*, *cis* and free ligands, respectively. These assignments are based on the relative intensities of the peaks in  $CDCl_3$  and  $CD_2Cl_2$ . Integration of the peaks confirms that the number of coordinated ligands is 2 and shows that the isomerization constant,  $K_{iso} = [trans]/[cis]$ , is 0.20 in  $CD_2Cl_2$ .

Tables III and IV contain the  $^1H$  and  $^{31}P\{^1H\}$  NMR results for the adducts with phosphoryl ligands. The  $^1H$  NMR spectrum of  $TiCl_4 \cdot 2TMPA$  in  $CHCl_3$  at 210 K shows three doublets (the doublets are due to  $^3J(^1H-^{31}P)$ ). The doublet centered at 3.84 ppm corresponds to free TMPA and the other two, centered at 4.11 and 4.25 ppm, are due to coordinated

TABLE III.  $^1\text{H}$  NMR Chemical Shifts  $\delta^a$ , Chemical Shift Differences  $\Delta\delta^b$  Coupling Constants, Stoichiometries, and Isomerization Constants<sup>c</sup> for the  $\text{TiX}_4 \cdot 2\text{L}$  Adducts with Phosphoryl Ligands in  $\text{CHCl}_3$  and  $\text{CH}_2\text{Cl}_2$ 

	$\text{TiCl}_4 \cdot 2\text{L}$ ( $\text{CHCl}_3$ )				$\text{TiBr}_4 \cdot 2\text{L}$ ( $\text{CH}_2\text{Cl}_2$ )	
	TMPA	$\text{Cl}(\text{MeO})_2\text{PO}$	$\text{Cl}_2(\text{Me}_2\text{N})\text{PO}$	$\text{Cl}(\text{Me}_2\text{N})_2\text{PO}$	$\text{Cl}_2(\text{Me}_2\text{N})\text{PO}$	$\text{Cl}(\text{Me}_2\text{N})_2\text{PO}$
<i>trans</i> - $\text{TiX}_4 \cdot 2\text{L}$						
$\delta \pm 0.01$ (ppm)	4.25			3.02		3.04
$\Delta\delta \pm 0.01$ (ppm)	0.41			0.25		0.33
$^3J(^1\text{H}-^{31}\text{P})$ (Hz) <sup>d</sup>	11.8			13.9		13.7
<i>cis</i> - $\text{TiX}_4 \cdot 2\text{L}$						
$\delta \pm 0.01$ (ppm)	4.11	4.22	3.09	2.94	3.06	2.93
$\Delta\delta \pm 0.01$ (ppm)	0.27	0.25	0.16	0.17	0.18	0.22
$^3J(^1\text{H}-^{31}\text{P})$ (Hz) <sup>d</sup>	11.8	14.6	16.5	13.7	16.7	13.5
Stoichiometry Ti:L	1:1.92	1:2.09	1:1.94	1:2.09	1:2.04	1:2.04
$K_{\text{iso}}$ ( $\text{CHCl}_3$ )	0.43			0.47		2.43
$K_{\text{iso}}$ ( $\text{CH}_2\text{Cl}_2$ )	0.17			0.21		1.21
$T$ (K)	210	204	205	231	183	262
$[\text{Ti}]_{\text{T}}$ ( $\text{mol kg}^{-1}$ )	0.10	0.067	0.10	0.10	0.10	0.10
$[\text{L}]_{\text{T}}$ ( $\text{mol kg}^{-1}$ )	0.40	0.27	0.40	0.40	0.46	0.40

<sup>a</sup>Internal reference was TMS. <sup>b</sup> $\Delta\delta = \delta(\text{TiCl}_4 \cdot 2\text{L}) - \delta(\text{L})$ . <sup>c</sup> $K_{\text{iso}} = [\text{trans-TiX}_4 \cdot 2\text{L}] / [\text{cis-TiX}_4 \cdot 2\text{L}]$ . <sup>d</sup>The free ligand coupling constant values (Hz) are: 11.1 for TMPA, 14.1 for  $\text{Cl}(\text{MeO})_2\text{PO}$ , 15.8 for  $\text{Cl}_2(\text{Me}_2\text{N})\text{PO}$  and 13.0 for  $\text{Cl}(\text{Me}_2\text{N})_2\text{PO}$ .

TABLE IV.  $^{31}\text{P}$  NMR Chemical Shifts  $\delta^a$  and Chemical Shift Differences  $\Delta\delta^b$  for  $\text{TiCl}_4 \cdot 2\text{L}$  in  $\text{CHCl}_3$ 

	TMPA	$\text{Cl}(\text{MeO})_2\text{PO}$	$\text{Cl}_2(\text{Me}_2\text{N})\text{PO}$	$\text{Cl}(\text{Me}_2\text{N})_2\text{PO}$
<i>trans</i> - $\text{TiCl}_4 \cdot 2\text{L}$				
$\delta \pm 0.01$ (ppm)	-4.8			31.8
$\Delta\delta \pm 0.01$ (ppm)	-6.9			0.6
<i>cis</i> - $\text{TiCl}_4 \cdot 2\text{L}$				
$\delta \pm 0.01$ (ppm)	-3.4	6.8	26.2	32.1
$\Delta\delta \pm 0.01$ (ppm)	-5.5	1.1	6.0	0.9
$T$ (K)	243	216	209	209
$[\text{Ti}]_{\text{T}}$ ( $\text{mol kg}^{-1}$ )	0.20	0.20	0.10	0.10
$[\text{L}]_{\text{T}}$ ( $\text{mol kg}^{-1}$ )	0.80	0.80	0.40	0.40

<sup>a</sup>External shift reference was 62.5%  $\text{H}_3\text{PO}_4$ . <sup>b</sup> $\Delta\delta = \delta(\text{TiCl}_4 \cdot 2\text{L}) - \delta(\text{L})$ .

forms of  $\text{TiCl}_4$ . To assign the coordinated peaks, the spectrum was also recorded in  $\text{CH}_2\text{Cl}_2$  and 1:1  $\text{CD}_3\text{NO}_2/\text{CH}_2\text{Cl}_2$ . These spectra are shown in Fig. 3. The intensity of the peaks at 4.11 ppm increase with increased solvent polarity and this allows us to assign them to the *cis* isomer and the ones at 4.25 ppm to the *trans* isomer. The relative shift of the *trans* signals with respect to the *cis* signals is the same as observed for solutions of  $\text{SnCl}_4 \cdot 2\text{TMPA}$  [6]. Integration of the peaks confirms the 1:2 stoichiometry and shows that  $K_{\text{iso}}$  decreases:  $K_{\text{iso}}$  is 0.43 in  $\text{CHCl}_3$ , 0.17 in  $\text{CH}_2\text{Cl}_2$  and 0.09 in 1:1  $\text{CD}_3\text{NO}_2:\text{CH}_2\text{Cl}_2$  at 210 K.

The isomerization constant varies in  $\text{CHCl}_3$  from 0.43 at 210 K to 0.36 at 277 K. This allows us to

determine the thermodynamic parameters  $\Delta H_{\text{iso}}^\circ$  and  $\Delta S_{\text{iso}}^\circ$  for the isomerization process from the temperature dependence of  $K_{\text{iso}}$ . We found that  $\Delta H_{\text{iso}}^\circ = -1.3 \pm 1.3$  kJ/mol and  $\Delta S_{\text{iso}}^\circ = -13.1 \pm 7.5$  J/mol K. The volume change for the isomerization,  $\Delta V_{\text{iso}}^\circ$ , was determined with variable pressure  $^1\text{H}$  NMR experiments in  $\text{CHCl}_3$  at 243 K. We measured  $\Delta V_{\text{iso}}^\circ$  to be  $-1.3 \pm 0.8$   $\text{cm}^3/\text{mol}$ ; the small negative value indicates that the *trans* isomer is slightly favored at elevated pressure.

For  $\text{TiCl}_4 \cdot 2\text{TMPA}$ , exchange was observed between the *cis* and free NMR signals beginning at 245 K, and at 320 K exchange was starting to occur between the *trans* signals and the coalesced *cis*/free signals.

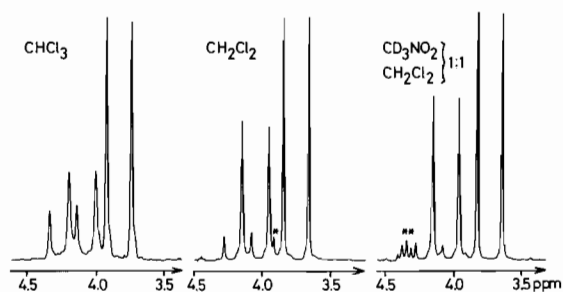


Fig. 3.  $^1H$  NMR spectra at 210 K of *cis*- and *trans*- $TiCl_4 \cdot 2TMPA$  in the presence of excess TMPA and in  $CHCl_3$ ,  $CH_2Cl_2$  and  $CD_3NO_2:CH_2Cl_2$  1:1.  $[TiCl_4 \cdot 2L] = 0.10$  mol  $kg^{-1}$ ,  $[free\ TMPA] = 0.2$  mol  $kg^{-1}$ . \*,  $^{13}C$  satellite of  $CH_2Cl_2$ ; \*\*,  $CHD_2NO_2$  solvent peaks.

TABLE V.  $^{19}F$  NMR Chemical Shifts  $\delta^a$ , Coupling Constants and Isomerization Constants $^b$  for  $TiF_4 \cdot 2L$  in  $CH_2Cl_2$

	TMPA	HMPA	Me <sub>3</sub> PO
<i>trans</i> - $TiF_4 \cdot 2L$			
$\delta$ (ppm)		135.3	132.9
<i>cis</i> - $TiF_4 \cdot 2L$			
$\delta_\alpha$ (ppm) <sup>c</sup>	146.6	131.7	128.4
$\delta_\beta$ (ppm)	215.5	184.7	180.4
$^2J(^{19}F_\alpha - ^{19}F_\beta)$ (Hz)	40.9	42.2	40.2
$K_{iso}$		0.08	0.04
$T$ (K)	248	300	248
$[Ti]_T$ (mol $kg^{-1}$ )	0.05	0.05	0.05
$[L]_T$ (mol $kg^{-1}$ )	0.40	0.40	0.20

<sup>a</sup>Internal shift reference was  $CFCl_3$ . <sup>b</sup> $K_{iso} = [trans-TiF_4 \cdot 2L] / [cis-TiF_4 \cdot 2L]$ . <sup>c</sup>The  $\alpha$  fluorines have been assigned as the ones *trans* to one another.

Three doublets were also observed in the  $^1H$  NMR spectra of the  $TiCl_4$  and  $TiBr_4$  adducts of  $Cl(Me_2N)_2PO$ . The signals were assigned in the same manner as for the  $TiCl_4 \cdot 2TMPA$  system and integration confirms the 1:2 stoichiometry. The isomerization constants are: for  $TiCl_4 \cdot 2Cl(Me_2N)_2PO$  at 231 K,  $K_{iso} = 0.47$  in  $CHCl_3$  and 0.21 in  $CH_2Cl_2$ ; for  $TiBr_4 \cdot 2Cl(Me_2N)_2PO$  at 262 K,  $K_{iso} = 2.43$  in  $CHCl_3$  and 1.21 in  $CH_2Cl_2$ . An increase in temperature resulted in exchange between *cis* and free ligands at 255 K for the  $TiCl_4$  adduct and at 273 K for the  $TiBr_4$  adduct. A second exchange involving the *trans* isomer was not observed for either adduct.

Only two doublets were present in the  $^1H$  NMR spectrum of the adducts  $TiCl_4 \cdot 2Cl(MeO)_2PO$ ,  $TiCl_4 \cdot 2Cl_2(Me_2N)PO$  and  $TiBr_4 \cdot 2Cl_2(Me_2N)PO$ . For the  $TiCl_4$  adducts the two peaks are assigned to the *cis* and free ligands since vibrational data indicate that only the *cis* form exists in solution. No vibrational data are available for the  $TiBr_4 \cdot 2Cl_2(Me_2N)PO$  adduct but we also assign this adduct as having only the *cis*

configuration due to the similarity of its chemical shifts to those of the  $TiCl_4$  analogue.

The  $^{19}F$  NMR spectra were recorded for three  $TiF_4 \cdot 2L$  adducts;  $L = TMPA, Me_3PO$  and HMPA (low solubility prevented extending the study to other  $TiF_4 \cdot 2L$  adducts). Table V summarizes the results and Fig. 4 shows the  $^{19}F$  NMR spectrum of  $TiF_4 \cdot 2HMPA$  at 300 K. *cis* and *trans* isomers are easily distinguished in  $^{19}F$  NMR since the equivalent *trans* fluorines give a single NMR signal and the inequivalent *cis* fluorines give a pair of triplets. The assignment of *cis*  $\alpha$  and *cis*  $\beta$  was based on the work of Dyer and Ragsdale [11] on complexes of the form  $TiF_4 \cdot L-L'$ .

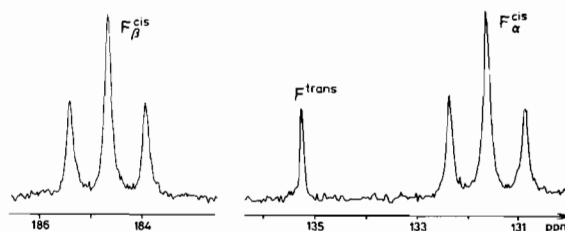


Fig. 4.  $^{19}F$  NMR spectrum at 300 K of *cis*- and *trans*- $TiF_4 \cdot 2HMPA$  in  $CH_2Cl_2$ . The  $\alpha$  fluorines of the *cis* isomer are those located in axial positions.

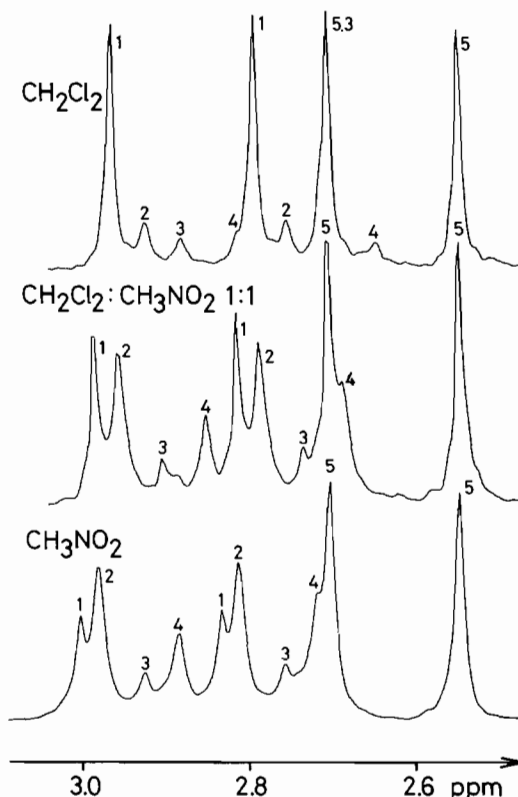


Fig. 5.  $^1H$  NMR spectra at 243 K of  $TiCl_4/HMPA$  in  $CH_2Cl_2$ ,  $CH_2Cl_2:CH_3NO_2$  1:1 and  $CH_3NO_2$ . Peak assignments are: 1, *trans*- $TiCl_4 \cdot 2HMPA$ ; 2,  $HMPA_\beta$  of  $[TiCl_3 \cdot 3HMPA]Cl$ ; 3, *cis*- $TiCl_4 \cdot 2HMPA$ ; 4,  $HMPA_\alpha$  of  $[TiCl_3 \cdot 3HMPA]Cl$ ; 5, free HMPA. See Fig. 6 for the assignment of  $HMPA_{\alpha,\beta}$ .

Vibrational spectroscopy data for the  $\text{TiCl}_4 \cdot 2\text{HMPA}$  adducts shows that only the *trans* isomer exists in solution in  $\text{CHBr}_3$ . However, the  $^1\text{H}$  NMR spectrum of this adduct in  $\text{CH}_2\text{Cl}_2$  shows 5 doublets, indicating a much more complicated system. The  $^1\text{H}$  NMR spectrum was also collected in 1:1  $\text{CH}_2\text{Cl}_2$ : $\text{CH}_3\text{NO}_2$  and in  $\text{CH}_3\text{NO}_2$ ; the spectra are shown in Fig. 5. Upon examination of the spectra we made the following assignment based on the behavior of the peaks in the three solvents and on the relative integrations. The peaks centered at 2.87, 2.79 and 2.62 ppm are assigned to the *trans*, *cis* and free HMPA, respectively. The doublets centered at 2.84 and 2.73 ppm have intensities of 2 to 1 and increase with solvent polarity but keep the same relative intensity of 2:1. We attribute the 2.84 and 2.73 signals as being due to the ionic species  $[\text{TiCl}_3 \cdot 3\text{HMPA}]\text{Cl}$  with the structure shown in Fig. 6. The overall stoichiometry from the integrations is 1:2.18 in  $\text{CHCl}_3$ , 1:2.24 in  $\text{CH}_2\text{Cl}_2$  and 1:2.53 in  $\text{CH}_3\text{NO}_2$  for a  $\text{TiCl}_4$  to HMPA ratio of 1:4. These high values imply that a species is formed with a coordination number greater than the usual two. The presence of an ionic species is supported by the conductivity of a 0.002 M solution in  $\text{CH}_3\text{NO}_2$ , for which a molar conductivity value of  $110 \text{ cm}^2 \Omega^{-1}$

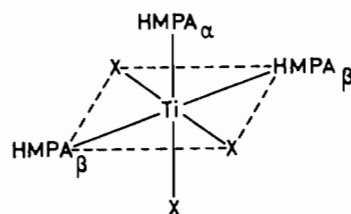


Fig. 6. Proposed structure of the cationic species  $[\text{TiX}_3 \cdot 3\text{HMPA}]^+$ , X = Cl, Br.

$\text{M}^{-1}$  was found, well within the values accepted for 1:1 electrolytes in  $\text{CH}_3\text{NO}_2$  ( $85\text{--}120 \text{ cm}^2 \Omega^{-1} \text{ M}^{-1}$ ) [12]. Table VI summarizes the results of the  $^1\text{H}$  and  $^{31}\text{P}\{^1\text{H}\}$  NMR experiments for the  $\text{TiCl}_4$  and  $\text{TiBr}_4$  adducts of HMPA. For the  $\text{TiBr}_4$  adduct only three doublets were observed and integration revealed that the stoichiometry was 1:2.92 in  $\text{CH}_2\text{Cl}_2$ , suggesting that the only species present is  $[\text{TiBr}_3 \cdot 3\text{HMPA}]\text{Br}$ . The ability of HMPA to compete with  $\text{Cl}^-$  and  $\text{Br}^-$  for coordination sites has been previously demonstrated for  $\text{TiX}_4$  adducts [13] and the formation of  $\text{Ti(III)Cl}_3 \cdot 3\text{HMPA}$  has also been reported [14].

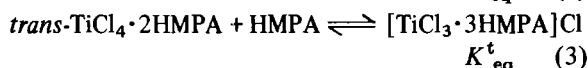
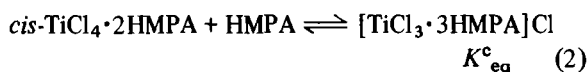
The following equilibria are observed for the  $\text{TiCl}_4/\text{HMPA}$  system:

TABLE VI.  $^1\text{H}$  and  $^{31}\text{P}\{^1\text{H}\}$  NMR Chemical Shifts  $\delta^a$ , Chemical Shift Differences  $\Delta\delta^b$ , Coupling Constants<sup>c</sup>, and Stoichiometries for  $\text{TiCl}_4 \cdot 2\text{HMPA}$  and  $[\text{TiX}_3 \cdot 3\text{HMPA}]\text{X}$  in  $\text{CH}_2\text{Cl}_2$

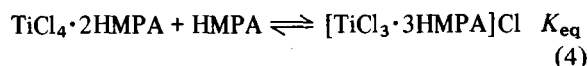
	X = Cl		X = Br	
	$^1\text{H}$ NMR	$^{31}\text{P}\{^1\text{H}\}$ NMR	$^1\text{H}$ NMR	$^{31}\text{P}\{^1\text{H}\}$ NMR <sup>e</sup>
<i>trans</i> - $\text{TiX}_4 \cdot 2\text{HMPA}$				
$\delta \pm 0.01$ (ppm)	2.87	27.3		
$\Delta\delta \pm 0.01$ (ppm)	0.25	2.6		
$^3J(^1\text{H}\text{--}^{31}\text{P})$ (Hz)	10.3			
<i>cis</i> - $\text{TiX}_4 \cdot 2\text{HMPA}$				
$\delta \pm 0.01$ (ppm)	2.79	27.6		
$\Delta\delta \pm 0.01$ (ppm)	0.17	2.9		
$^3J(^1\text{H}\text{--}^{31}\text{P})$ (Hz)	10.2			
$[\text{TiX}_3 \cdot 3\text{HMPA}]\text{X}$				
$\delta_\alpha \pm 0.01$ (ppm) <sup>d</sup>	2.73	26.3	2.73	27.0
$\Delta\delta_\alpha \pm 0.01$ (ppm)	0.11	1.6	0.11	1.0
$^3J(^1\text{H}\text{--}^{31}\text{P})$ (Hz) <sup>d</sup>	9.8		10.0	
$\delta_\beta \pm 0.01$ (ppm)	2.84	27.1	2.89	27.8
$\Delta\delta_\beta \pm 0.01$ (ppm)	0.22	2.4	0.27	1.8
$^3J(^1\text{H}\text{--}^{31}\text{P})$ (Hz) <sup>d</sup>	10.2		10.0	
Stoichiometry Ti:L	1:2.24		1:2.92	
$[\text{Ti}]_T$ (mol kg <sup>-1</sup> )	0.10	0.10	0.067	0.10
$[\text{L}]_T$ (mol kg <sup>-1</sup> )	0.40	0.40	0.27	0.40
T (K)	243	213	243	213

<sup>a</sup>For  $^1\text{H}$  NMR the internal shift standard was TMS. For  $^{31}\text{P}\{^1\text{H}\}$  NMR the external shift standard was 62.5%  $\text{H}_3\text{PO}_4$ . <sup>b</sup> $\Delta\delta = \delta(\text{coordinated HMPA}) - \delta(\text{free HMPA})$ . <sup>c</sup> $^3J(^1\text{H}\text{--}^{31}\text{P})$  for the free HMPA was 9.3 Hz. <sup>d</sup>HMPA<sub>α</sub> has been defined as the ligand *trans* to a halogen (see Fig. 6). <sup>e</sup>In  $\text{CDCl}_3$ .





If we let  $[\text{TiCl}_4 \cdot 2\text{HMPA}]$  equal the sum of the *cis* and *trans*- $\text{TiCl}_4 \cdot 2\text{HMPA}$  adducts, one can describe the formation of the cationic species by the equilibrium:



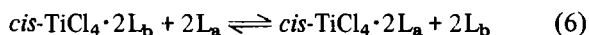
Combination of the equilibria (1) to (3) and (2) to (4), respectively, using the law of mass action gives:

$$K_{iso} = K_{eq}^c / K_{eq}^t \quad \text{and} \quad 1/K_{eq} = 1/K_{eq}^c + 1/K_{eq}^t \quad (5)$$

The results from a quantitative study on the above equilibria using  $^1\text{H}$  NMR are summarized in Table VII. The results show that in a low polarity solvent with a small excess of ligand the predominating species in solution is *trans*, which explains the observations in the vibrational experiments in  $\text{CHBr}_3$ . As the solvent polarity increases,  $K_{iso}$  decreases.  $K_{eq}$  also decreases but stabilizes at a  $\text{CH}_2\text{Cl}_2/\text{CH}_3\text{NO}_2$

mixture of 40:60. Equation (5) shows that in the solvent mixtures where  $K_{eq}$  is constant,  $K_{eq}^t$  continues to increase with solvent polarity while  $K_{eq}^c$  decreases, showing that the *cis* isomer is favored in more polar media.

Proton NMR was used to estimate the relative stability of the *cis*- $\text{TiCl}_4 \cdot 2L$  adducts by considering the equilibrium:



for which the equilibrium constant expression is

$$K_{a,b} = \frac{[cis\text{-TiCl}_4 \cdot 2L_a][L_b]^2}{[cis\text{-TiCl}_4 \cdot 2L_b][L_a]^2} \quad (7)$$

The stability constants were determined by integration of the NMR signals at a temperature where ligand exchange is negligible. For systems which have mixed ligand species, *cis*- $\text{TiCl}_4 \cdot L_a \cdot L_b$ , the concentration of the *cis*- $\text{TiCl}_4 \cdot 2L$  adducts cannot be determined independently from the mixed species. For these systems the stability constants were estimated as described by Ruzicka and Merbach [6] for the analogous  $\text{SnCl}_4 \cdot 2L$  adducts. Table VIII contains the

TABLE VII. Equilibrium Constants for the  $\text{TiCl}_4/\text{HMPA}$  System as a Function of Free HMPA Concentration and Solvent Composition at 243 K.  $[\text{Ti}]_T = 0.10 \text{ mol kg}^{-1}$

Solvent	[HMPA] <sup>a</sup> (mol kg <sup>-1</sup> )	$\chi^b$	$K_{eq}^c$	$K_{iso}^d$
$\text{CHCl}_3$	0.21	0.19	0.021	9.1
$\text{CH}_2\text{Cl}_2$	0.07	0.12	0.023	6.1
$\text{CH}_2\text{Cl}_2$	0.15	0.17	0.023	6.3
$\text{CH}_2\text{Cl}_2$	0.36	0.25	0.023	6.5
$\text{CH}_2\text{Cl}_2$	0.53	0.29	0.022	6.1
$\text{CH}_2\text{Cl}_2/\text{CH}_3\text{NO}_2$ 80:20	0.13	0.30	0.10	4.6
$\text{CH}_2\text{Cl}_2/\text{CH}_3\text{NO}_2$ 60:40	0.11	0.42	0.28	3.2
$\text{CH}_2\text{Cl}_2/\text{CH}_3\text{NO}_2$ 50:50	0.13	0.46	0.30	3.1
$\text{CH}_2\text{Cl}_2/\text{CH}_3\text{NO}_2$ 40:60	0.094	0.45	0.39	3.0
$\text{CH}_2\text{Cl}_2/\text{CH}_3\text{NO}_2$ 20:80	0.13	0.50	0.38	2.4
$\text{CH}_3\text{NO}_2$	0.15	0.53	0.40	1.8

<sup>a</sup> Determined by integration of the  $^1\text{H}$  NMR signals. <sup>b</sup>  $\chi = \text{mole fraction } [\text{TiCl}_3 \cdot 3\text{HMPA}]\text{Cl} = ([\text{TiCl}_3 \cdot 3\text{HMPA}]\text{Cl})/[\text{Ti}]_T$ .  
<sup>c</sup>  $K_{eq} = ([\text{TiCl}_3 \cdot 3\text{HMPA}]^+)[\text{Cl}^-]/[cis\text{- and } trans\text{-TiCl}_4 \cdot 2\text{HMPA}][\text{HMPA}]$ . <sup>d</sup>  $K_{iso} = [trans\text{-TiCl}_4 \cdot 2\text{HMPA}]/[cis\text{-TiCl}_4 \cdot 2\text{HMPA}]$ .

TABLE VIII. Estimated Relative Stability Constants for the *cis*- $\text{TiCl}_4 \cdot 2L$  Adducts<sup>a</sup> in  $\text{CH}_2\text{Cl}_2$  at 181 K

$L_a$	$L_b$	$K_{a,b}$	$L_c$	$K'_{a,b}{}^b$	$\log K''_{a,b}{}^c$
$\text{Cl}(\text{Me}_2\text{N})_2\text{PO}$	TMPA	36			1.56
$\text{Me}_2\text{Se}$	$\text{Me}_2\text{S}$	1.8			0.25
$\text{Me}_2\text{S}$	MeCN	72			1.86
	$\text{Me}_2\text{O}$	112	MeCN	100	2.03
$\text{Me}_2\text{CO}$	MeCN	9.1			0.96
	$\text{Me}_2\text{O}$	12.5	MeCN	12.6	1.10
MeCN	$\text{Me}_2\text{O}$	1.38			0.14

<sup>a</sup>  $[\text{TiCl}_4]_T = 0.05\text{--}0.10 \text{ mol kg}^{-1}$ ,  $[L_a]_T + [L_b]_T = 0.30\text{--}1.0 \text{ mol kg}^{-1}$ . <sup>b</sup>  $K'_{a,b} = K_{a,c} \times K_{c,b}$ . <sup>c</sup>  $K''_{a,b}$  = average value of  $K_{a,b}$ .

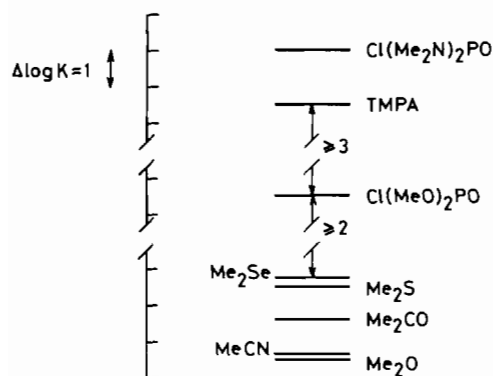


Fig. 7. Relative stabilities of the *cis*-TiCl<sub>4</sub>·2L adducts as determined by NMR. The measurements were made in CH<sub>2</sub>Cl<sub>2</sub> at 181 K. [TiCl<sub>4</sub>]<sub>T</sub> = 0.05–0.10 mol kg<sup>-1</sup>.

results of the stability constant determination in CH<sub>2</sub>Cl<sub>2</sub> at 181 K. Whenever possible, the values of  $K_{a,b}$  were checked by using the thermodynamic relationship  $K'_{a,b} = K_{a,c} \times K_{c,b}$ . The results, pictured in Fig. 7, show that the stability of the complexes increases in the order Me<sub>2</sub>O ~ MeCN < Me<sub>2</sub>CO < Me<sub>2</sub>S < Me<sub>2</sub>Se ≪ Cl(MeO)<sub>2</sub>PO ≪ TMPA < Cl(Me<sub>2</sub>N)<sub>2</sub>PO.

## Discussion

### Stability of the Adducts

The *cis*-TiCl<sub>4</sub>·2L adducts with dimethylchalcogen ligands have the same sequence of stability as observed for *cis*- and *trans*-SnCl<sub>4</sub>·2L [6] and MX<sub>5</sub>·L (M = Nb, Ta) [15, 16] adducts: Me<sub>2</sub>Se > Me<sub>2</sub>S ≫ Me<sub>2</sub>O. This stability sequence provides the basis for classifying TiCl<sub>4</sub> according to hard soft acid base theory (HSAB). The small, highly charged Ti<sup>4+</sup> ion is considered to be a hard acid [17]. The fact that we obtained more stable adducts with the soft Se and S donors than with the hard O donor suggests that TiCl<sub>4</sub> is a soft acid. The enthalpies of formation for several TiCl<sub>4</sub>·2L adducts have been determined and these data show that the hard O atom in THF ( $\Delta H_f = -194$  kJ/mol) is a stronger coordinator than the soft S donor in THT ( $\Delta H_f = -117$  kJ/mol) [18]. Vibrational measurements have shown that the Ti–L bond in thioxane and selenoxane adducts of TiCl<sub>4</sub> and TiBr<sub>4</sub> is preferentially made through the soft S or Se atoms over the hard oxygen atoms [19], showing the soft acid behaviour of TiCl<sub>4</sub>. A study of TiCl<sub>4</sub> with potentially terdentate tripod ligands of the type CH<sub>3</sub>C(X)(Y)(Z) in which X, Y, Z can be CH<sub>2</sub>OMe, CH<sub>2</sub>SMe or CH<sub>2</sub>NMe<sub>2</sub> has been reported [20]. The authors observed that these ligands are bidentate towards TiCl<sub>4</sub> and that coordination is made through the hard N atom over the soft S or hard O atoms and also that if a site is initially N bonded the second site

will be occupied by O rather than S. These studies emphasize that TiCl<sub>4</sub> is a softer acid than its position in the Periodic Table would imply. This supports the symbiotic effect proposed by Jørgensen [21] in 1964 in which it was proposed that the hardness of a Lewis acid will decrease when it is bonded to progressively softer Lewis bases. This implies that TiBr<sub>4</sub> should be a softer acid than TiCl<sub>4</sub>. Because of the formation of mixed TiCl<sub>x</sub>Br<sub>4-x</sub>·2L species we were unable to determine the relative stability of TiBr<sub>4</sub> adducts with respect to those of TiCl<sub>4</sub>. However, support for the prediction is given by the fact that formation of 1:2 adducts of TiBr<sub>4</sub> with hard Lewis bases such as MeCN and Me<sub>2</sub>CO was not complete. Our stability scale, Fig. 7, shows that the phosphoryl ligands form the most stable TiCl<sub>4</sub> adducts. The donor strength of phosphoryl ligands is very dependent on the electron donating or withdrawing ability of the ligand substituents [22]. This is demonstrated in the stability scale since the ligands containing electron withdrawing Cl atoms are less stable than those that contain the electron donating MeO and Me<sub>2</sub>N groups.

### Adduct Structure

The TiCl<sub>4</sub>·2L adducts can exist in two isomeric forms: *cis* and *trans*. Since *cis* and *trans* isomers are not formed equally for all adducts, various factors have been suggested as being influential in the formation of one isomer over the other. A stereochemical model has been proposed for TiCl<sub>4</sub>·2L adducts based on van der Waals interactions of the donor atoms in the coordination sphere of the adduct [23]. This model neglects electronic and secondary bonding effects and when it is applied to the adducts studied in this work it predicts that the *cis* isomer is favored for all the adducts. Another sterical approach to the problem considered the relative sizes of the halogens in TiX<sub>4</sub> and of the donor atom of the ligands [24]. This model predicts that when the halogen is larger than the donor atom, the *cis* isomer is favored over the *trans* since the four halogen atoms can rearrange to reform the pseudo-tetrahedral structure for the halogens, which decreases the steric interactions between the halogens. Conversely, if the donor atom of the ligand is larger than the halogen or if the ligand is strongly sterically hindered, ligand–halogen and ligand–ligand interactions will predominate over halogen–halogen interactions and the *trans* isomer will be favored. These models only consider steric interactions between the various atoms in the inner coordination sphere of the adduct. It has been shown that for the analogous SnX<sub>4</sub>·2L [6] complexes both *cis* and *trans* isomers exist for adducts containing Lewis base ligands which only form the *cis* isomer in TiX<sub>4</sub>·2L. Since *trans*-SnX<sub>4</sub>·2L isomers are more readily formed than *trans*-TiX<sub>4</sub>·2L isomers, models based only on steric interactions cannot be correct because the diameters of SnCl<sub>4</sub> and TiCl<sub>4</sub> are similar.

TABLE IX. Isomerization Constants,  $K_{iso} = [trans]/[cis]$ , for the  $TiX_4 \cdot 2L$  Adducts in  $CH_2Cl_2$ 

	Me <sub>3</sub> PO	HMPA	Cl(Me <sub>2</sub> N) <sub>2</sub> PO	TMPA	THF
TiF <sub>4</sub> ·2L	0.04	0.08	<sup>a</sup>	0	<sup>a</sup>
TiCl <sub>4</sub> ·2L	<sup>b</sup>	6.3 <sup>c</sup>	0.21	0.17	0.20
TiBr <sub>4</sub> ·2L	<sup>b</sup>	<sup>d</sup>	1.21	<sup>b</sup>	<sup>a</sup>

<sup>a</sup>The complex was not made. <sup>b</sup>The complex precipitated or decomposed on formation. <sup>c</sup>This solution also contains the complex  $[TiCl_3 \cdot 3HMPA]Cl$ . <sup>d</sup>This solution contained only  $[TiBr_3 \cdot 3HMPA]Br$ .

The determining factor in the formation of  $TiX_4 \cdot 2L$  isomers seems to be the  $p_\pi-d_\pi$  overlap between the filled 2p orbitals of the halogen atoms and the empty  $t_{2g}$  orbitals of titanium [5, 25]. The halogen atoms in the  $TiX_4$  adducts compete for the available Ti  $d_\pi$  orbitals with the ligand bonded *trans* to it and our data show that the halogens will arrange themselves into a position to maximize X-Ti  $p_\pi-d_\pi$  bonding. If the Lewis base ligand is a worse  $\pi$  electron donor than the halogen, the latter will preferentially have the Lewis base in the *trans* position with respect to itself since there will be a weaker competition for  $\pi$ -overlap with the Ti  $t_{2g}$  orbitals. If the ligands contain bulky constituents then steric interactions will be large enough to overcome the  $p_\pi-d_\pi$  bonding effects and the adduct will be of a configuration in which the van der Waals interactions between the various atoms will be reduced. Therefore, the geometry of  $TiX_4 \cdot 2L$  adducts is determined by X-Ti  $p_\pi-d_\pi$  bonding interactions except when the adduct contains bulky ligands. The  $p_\pi-d_\pi$  interactions appear to be unimportant in the formation of the  $d^{10}$   $SnX_4 \cdot 2L$  adducts.

Considering the factors which influence the configuration of  $TiX_4 \cdot 2L$  adducts, steric interactions and  $p_\pi-d_\pi$  bonding, we would expect most of the adducts in this study to have the *cis* configuration since they are, for the most part, weak  $\pi$  donors and relatively unhindered. This was observed. Some of the systems did have the *trans* isomer present but these systems contained Lewis base ligands with good  $\pi$ -donating ability.

For systems containing a *cis-trans* equilibrium, the isomerization constants are given in Table IX. It appears that the proportion of *trans* to *cis* increases as the small fluorine atoms are replaced with larger chlorine and larger yet bromine atoms, reflecting the importance of steric interactions. Also, the proportion of *trans* to *cis* seem to increase with the donor strength of the Lewis base ligand, showing the importance of  $p_\pi-d_\pi$  bonding effects.

The effect of pressure on the *cis-trans* isomerization constant for  $TiCl_4 \cdot 2TMPA$  in  $CHCl_3$  was found to give a  $\Delta V_{iso}^\circ$  of  $-1.3 \pm 0.8$  cm<sup>3</sup>/mol, or near zero. The small negative value means that the *trans* isomer is slightly favored over the *cis* at elevated pressure. For *cis/trans*- $SnCl_4 \cdot 2Me_2S$  in  $CH_2Cl_2$ ,  $\Delta V_{iso}^\circ$  is

$+3.2 \pm 0.4$  cm<sup>3</sup>/mol [4]. The stabilization of one isomer over another at elevated pressure depends on several, often competing, effects. The *cis* adduct has a small but nonzero dipole moment so electrostriction will be more appreciable on the *cis* isomer than on the *trans*. This explained why *cis*- $SnCl_4 \cdot 2Me_2S$  was more favored at higher pressure than *trans*- $SnCl_4 \cdot 2Me_2S$ . This effect is not observed for  $TiCl_4 \cdot 2TMPA$ , probably because TMPA is a much larger ligand than  $Me_2S$  and the magnitude of the electrostriction decreases with an increase in the size of the dipolar molecule.

In conclusion, *cis-trans* isomerization for  $TiX_4 \cdot 2L$  adducts in solution is only important for those adducts which contain strong Lewis base ligands or ligands with a large amount of bulk. Moreover, for those adducts containing phosphoryl ligands the isomerization constant increases with the donor strength of the phosphoryl group. An increase in the proportion of the *trans* isomer with respect to the ligand base strength has also been observed for a series of  $TiF_4 \cdot 2L$  adducts where L is a number of substituted quinoline oxides [26]. The connection between strong ligand-metal bonds and the formation of the *trans* isomer is supported by the structure of the ionic complex  $[TiX_3 \cdot 3HMPA]X$  where only the isomer with two HMPA ligands located *trans* to each other has been detected; the other structure with all HMPA ligands located *trans* to halogen atoms has not been observed.

### Acknowledgement

This work was financially supported by the Swiss National Science Foundation (Grant No. 2.854-0.85).

### References

- 1 Y. Ducommun and A. E. Merbach, in R. van Eldik (ed.), 'Inorganic High Pressure Chemistry, Kinetics and Mechanisms', Elsevier, Amsterdam, 1986, Chap. 2.
- 2 H. Vanni and A. E. Merbach, *Inorg. Chem.*, **18**, 2758 (1979).
- 3 J.-E. Kessler, C. T. G. Knight and A. E. Merbach, *Inorg. Chim. Acta*, **115**, 85 (1986).
- 4 C. T. G. Knight and A. E. Merbach, *Inorg. Chem.*, **24**, 576 (1985).

- 5 D. S. Dyer and R. O. Ragsdale, *Inorg. Chem.*, **8**, 1116 (1969).
- 6 S. J. Ruzicka and A. E. Merbach, *Inorg. Chim. Acta*, **20**, 221 (1976) and **22**, 191 (1977).
- 7 C. Ammann, P. Meier and A. E. Merbach, *J. Magn. Reson.*, **46**, 319 (1982).
- 8 D. L. Pisaniello, L. Helm, P. Meier and A. E. Merbach, *J. Am. Chem. Soc.*, **105**, 4528 (1983).
- 9 I. R. Beattie, M. Webster and G. W. Chantry, *J. Chem. Soc.*, 6172 (1964).
- 10 L. K. Tan and S. Brownstein, *Inorg. Chem.*, **23**, 1353 (1984).
- 11 D. S. Dyer and R. O. Ragsdale, *Inorg. Chem.*, **6**, 8 (1967).
- 12 W. J. Geary, *Coord. Chem. Rev.*, **7**, 81 (1971).
- 13 A. I. Kuzmin and S. I. Kuznetsov, *Soviet J. Coord. Chem. (Engl. Transl.)*, **8**, 81 (1983).
- 14 S. R. Wade and G. R. Willey, *J. Inorg. Nucl. Chem.*, **42**, 1133 (1980).
- 15 A. E. Merbach and J.-C. G. Bünzli, *Helv. Chim. Acta*, **55**, 580 (1972).
- 16 R. Good and A. E. Merbach, *Helv. Chim. Acta*, **57**, 1192 (1974).
- 17 R. G. Pearson, *J. Chem. Educ.*, **45**, 581 and 643 (1968).
- 18 B. Hessel and P. G. Perkins, *J. Chem. Soc. A*, 3229 (1970).
- 19 K. L. Baker and G. W. A. Fowles, *J. Chem. Soc. A*, 801 (1968).
- 20 A. J. McAlees, R. McCrindle and A. R. Woon-Fat, *Inorg. Chem.*, **15**, 1065 (1976).
- 21 C. K. Jørgensen, *Inorg. Chem.*, **3**, 1201 (1964).
- 22 E. L. Wagner, *J. Am. Chem. Soc.*, **85**, 161 (1963).
- 23 R. F. Zahrobsky, *J. Coord. Chem.*, **1**, 301 (1971).
- 24 I. R. Beattie, *Q. Rev.*, **17**, 382 (1963).
- 25 R. S. Borden and R. N. Hammer, *Inorg. Chem.*, **9**, 2004 (1970); R. S. Borden, P. A. Loeffler and D. S. Dyer, *Inorg. Chem.*, **11**, 2481 (1972).
- 26 C. E. Michelson, D. S. Dyer and R. O. Ragsdale, *J. Chem. Soc. A*, 2296 (1970).
- 27 I. V. Ikonitskii, N. A. Buzina, L. K. Kurnosova and E. N. Kropacheva, *Zh. Prikl. Spektrosk.*, **34**, 673 (1981).
- 28 I. R. Beattie and M. Webster, *J. Chem. Soc.*, 3507 (1964).
- 29 E. Lecoz and J. E. Guerchais, *Bull. Soc. Chim. Fr.*, **1**, 80 (1971).
- 30 S. R. Wade and G. R. Willey, *J. Inorg. Nucl. Chem.*, **42**, 1133 (1980).
- 31 H. S. Ahuja, S. C. Jain and R. Rivest, *J. Inorg. Nucl. Chem.*, **30**, 2459 (1968).